

Accepted Manuscript

Stereochemical correction and total structure of roridin J

Manami Matsumoto, Atsushi Ito, Akio Tonouchi, Masaaki Okazaki, Masaru Hashimoto



PII: S0040-4020(17)30790-1

DOI: [10.1016/j.tet.2017.07.048](https://doi.org/10.1016/j.tet.2017.07.048)

Reference: TET 28880

To appear in: *Tetrahedron*

Received Date: 22 June 2017

Revised Date: 25 July 2017

Accepted Date: 26 July 2017

Please cite this article as: Matsumoto M, Ito A, Tonouchi A, Okazaki M, Hashimoto M, Stereochemical correction and total structure of roridin J, *Tetrahedron* (2017), doi: 10.1016/j.tet.2017.07.048.

This is a PDF file of an unedited manuscript that has been accepted for publication. As a service to our customers we are providing this early version of the manuscript. The manuscript will undergo copyediting, typesetting, and review of the resulting proof before it is published in its final form. Please note that during the production process errors may be discovered which could affect the content, and all legal disclaimers that apply to the journal pertain.

Graphical Abstract

To create your abstract, type over the instructions in the template box below.
Fonts or abstract dimensions should not be changed or altered.

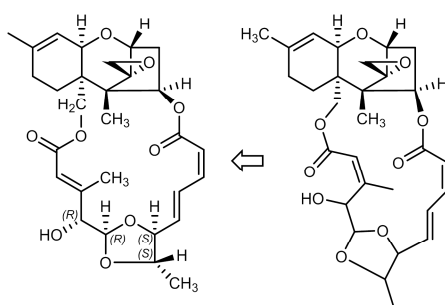
Stereochemical Correction and Total Structure of Roridin J

Leave this area blank for abstract info.

Manami Matsumoto,^a Atsushi Ito,^a Akio Tonouchi,^a
Masaaki Okazaki,^b and Masaru Hashimoto^{a,*}

^a Faculty of Agriculture and Life Science, Hirosaki University, 3-Bunkyo-cho, Hirosaki, 036-8561, Japan

^b Graduate School of Science and Technology, Hirosaki University, 3-Bunkyo-cho, Hirosaki, 036-8561, Japan



ACCEPTED MANUSCRIPT



Stereochemical Correction and Total Structure of Roridin J

Manami Matsumoto,^a Atsushi Ito,^a Akio Tonouchi,^a Masaaki Okazaki,^b and Masaru Hashimoto^{a,*}

^a Faculty of Agriculture and Life Science, Hirosaki University, 3-Bunkyo-cho, Hirosaki, 036-8561, Japan

^b Graduated School of Science and Technology, Hirosaki University, 3-Bunkyo-cho, Hirosaki, 036-8561, Japan

ARTICLE INFO

Article history:

Received

Received in revised form

Accepted

Available online

Keywords:

roridin J

verrucarol

structural revision

modeling calculation

theoretical spectra

ABSTRACT

The (2'Z)-configuration of roridin J (**1**) was revised to the (2'E) form by conducting NOE experiments. Although the configurations with respect to the stereogenic carbons on the macrocyclic ring of **1** had remained unknown, a combination of NMR analysis and molecular modeling calculations revealed the (2'E,5'R,6'S,7'E,9'Z,13'S) form. In addition, the modeling calculations successfully reproduced the ¹H and ¹³C NMR chemical shifts and the ECD spectrum. An X-ray crystallographic analysis verified all the relative configurations.

2009 Elsevier Ltd. All rights reserved.

1. Introduction

Trichothecenes carrying macrocyclic rings, such as roridins,^{1,2} verrucarins, baccharins,^{3,4} and muconomycins⁵, have been isolated from fungal sources, such as the *Myrothecium* and *Fusarium* species. In addition to unique structures, these exhibit potent antifungal,^{6,7} lethal,⁸ and/or cytotoxic⁹⁻¹¹ properties. Accordingly, this family has attracted attention of the organic chemists and biological scientists.^{1,12,13} Although a comprehensive biological investigation requires well-established three-dimensional structures, the configurations of the macrocyclic moiety in some roridin congeners, e.g., roridin J (**1**) were not determined (**Figure 1**). While exploring the fungal secondary metabolites, we had an opportunity to isolate **1** from *Calcarisporium arbuscular*, which led us to fully determine its stereostructure using a combination of spectral analysis and molecular modeling calculations. We succeeded in not only revising the configuration of the C2'C3' double bond but also establishing all configurations of asymmetric centers on the macrocycles. The proposed configuration was confirmed by an X-ray crystallographic diffraction analysis.

2. Results and discussion

Roridin J (**1**) was isolated from the culture broth of *C. arbuscula*. The ¹³C NMR spectral data of our sample were coincident with those reported by Jarvis in 1980 (max |Δδ¹³C|: 0.1 ppm, both in CDCl₃).¹⁴ Although Jarvis reported a potent NOE between H₃-12' and H-2' to conclude the (2'Z) form for the original structure of roridin J (**1'**), irradiation of H-2' resulted a remarkable signal enhancement at H-4' (13%) in our experiment, while that at H₃-12' was not obvious (1.3%), as shown in **Figure**

2. This result allowed us to revise that into the (2'E) configuration shown as **1**. The chemical shift for C12' (13.26 ppm) supported our revision by taking account of the steric compression effect due to the C1' carbonyl group.¹⁵ Methyl carbons on the trisubstituted Z-double bonds usually resonate at 22–27 ppm, while those of corresponding E-isomers appear at around 5–10 ppm lower frequency. This was further verified through chemical shift calculations, as described later.

Although several trichothecenes carrying macrocyclic rings have been reported, there is a poor consistency in the configurations of the stereogenic centers on the macrocycles; e.g., four diastereomers at C6' and C13' are known as roridin E and its analogs [only epiisororidin E (**2**) is shown in **Figure 1**].¹⁶ As the configurations C4', C5', C6', and C13' of **1** are unknown,

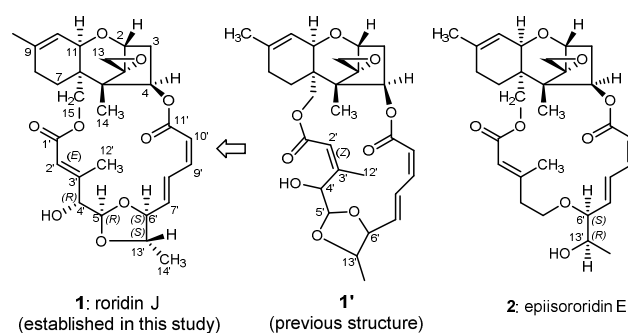


Figure 1. Structures of roridin J (**1**), its original structure (**1'**), and

isolation of **1** allows us to experimentally deduce them.

Prior to these investigations, the relative and absolute

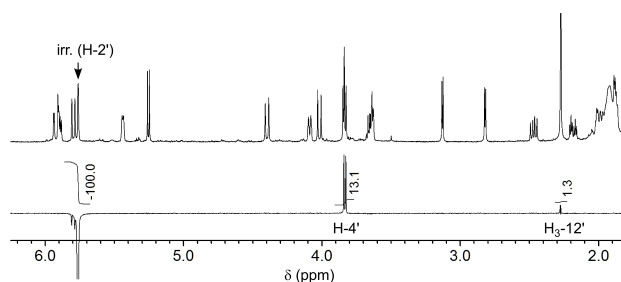
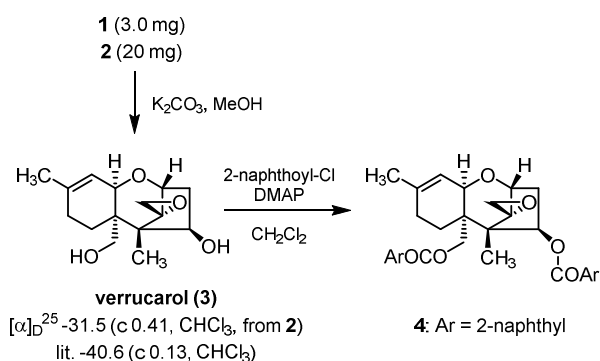


Figure 2. Medium-frequency region of the difference NOE spectrum of **1** obtained by irradiating H-2'.

configurations of the C1–C16 trichothecene moiety were experimentally confirmed. The NOESY spectrum afforded the correlations at H α -3/H-4, H α -3/H-11, H-4/H-11, H-4/H-14, H-4/H-15, and H β -7/H-13, indicating that the relative stereochemistry of trichothecene part is identical to those of other roridins.^{17,18,11} The absolute configuration of this moiety was established by a chemical correlation with verrucarol (**3**)^{19,20} being obtained by a basic methanolysis of **1**. Crude sample **3** thus prepared (1.5 mg) provided an ¹H NMR spectrum that showed accordance with the data in the literature;¹⁹ however, it was both qualitatively and quantitatively insufficient for measuring the specific rotation. It was found that the following derivatization into bis-*O*-2-naphthoate **4** resulted in giving distinct Cotton effects at 242 ($\Delta\epsilon$ +6.8) and 229 nm ($\Delta\epsilon$ –20.2) in the ECD spectrum after purification with preparative silica gel TLC. Fortunately, the producer fungus *C. arbuscula* afforded a considerable amount of **2**, a congener carrying the same trichothecene unit.¹⁶ Basic methanolysis of **2** under the same abovementioned conditions afforded authentic **3** (4.5 mg), which allowed us to obtain a reliable specific rotation ($[\alpha]_D^{22}$ –31.5 (c



Scheme 1. Chiral assignment of the trichothecene part.

0.41, CHCl₃). The following 2-naphthoylation afforded **4**, which gave identical ECD spectrum to that of the sample prepared from **1**. Ishihara and Tadano synthesized verrucarol in an optically active form to report its specific rotation ($[\alpha]_D^{21}$ –40.6 (c 0.13, CHCl₃)).^{19,20} A combination of these results established the absolute configuration for the trichothecene moiety in **1**, despite the indirect manner.

The vicinal spin couplings ³J_{H-7'/H-8'} (15.0 Hz) and ³J_{H-9'/H-10'} (11.1 Hz) confirm the same (7'*E*,9'*Z*) form as Jarvis's assignment. The NOESY spectrum affords a correlation between H-7' and H-9', suggesting a *transoid* conformation for the C7'–C10' diene

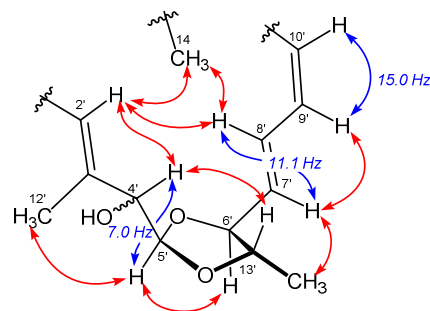


Figure 3. Relative configuration of the macrocyclic moiety and the characteristic NOEs as well as the ¹H coupling constants.

moiety as shown in **Figure 3**. In addition, NOESY correlations are found at H-4'/H-13' and H-5'/H-6', establishing a *rel*-(5'*R*,6'*S*,13'*S*) configuration of the 1,3-dioxolane ring moiety on the macrocycle.

The remaining structural unknowns were the absolute configurations of C4' and C5', which were investigated with the stable conformation, theoretical ¹H and ¹³C chemical shifts, and ECD spectrum based on DFT ω B97X-D/6-31G* (structural optimization and chemical shift calculations) and B3LYP/def2-TZVP// ω B97X-D/6-31G* (ECD spectral calculations) by using a protocol similar to that used in previous studies.^{21,22} Since the macrocyclic part of **1** has high conformational flexibility, the conformational distribution was estimated based on the free energy (*G*) by adding the entropic factor (*S*) and the temperature term (298 K) to the steric energy (*H*). The δ C and δ H root-mean-square (RMS) values of each isomer were obtained from the residuals between the experimental and theoretical chemical shifts. As we have established the *rel*-(5'*R*,6'*S*,13'*S*) configuration and the (2'*E*,7'*E*,9'*Z*) geometry via NMR analysis, the (4'*R*) and (4'*S*) epimers of both (2'*E*,5'*R*,6'*S*,7'*E*,9'*Z*,13'*S*) and (2'*E*,5'*S*,6'*R*,7'*E*,9'*Z*,13'*R*) forms (in total, four isomeric models) were subjected to the calculations. The models are expressed using three letters, e.g., **ERR**, and these three letters refer to the configurations at the 2',3' double bond, the 4', and 5' asymmetric carbons.

The calculations naturally revealed the stable conformers as shown in **Figure 4**. First, we analyzed the transannular NOEs based on their stable conformers suggested by these calculations. Roridin J (**1**) shows transannular NOEs at H₃-14/H-2', H₃-14/H-8', H-2'/H-8', and H-4'/H-13'. The most stable conformer of model **ERR** explains all these NOEs. Since C4'-epimeric model **ESR** adopts the similar conformation on the basis of these calculations, this isomer would also satisfy most of the above NOEs; however, the distance between H-4' and H-13' (3.6 Å) is slightly large to expect a distinct NOE between those (note that the distance between the vicinal *trans*-diaxial protons on a chair formed cyclohexane is around 3.1 Å). The calculations also revealed that the C1'–C4'-conjugated planes in the stable conformers of models **ERS** and **ESS** are flipped around from that in model **ERR**, which increased the distance between H₃-14 and H-2' (**ERS**: 4.2 Å and **ESS**: 4.0 Å). Thus, the NOE between these protons cannot be expected in those models. The characteristic difference between the stable conformers of models **ERR** and **ESR** is the dihedral angle H-4'/H-5'. These hydrogen atoms adopt a nearly antiperiplanar relationship in the stable conformers of model **ERR**, while these in model **ESR** is synclinal. The Boltzmann distribution weighted ³J_{H-4'/H-5'} value of model **ERR** is 5.9 Hz (**Table A** in **Figure 5**) which is in agreement with the experimental coupling constant of 7.0 Hz, when the ³J_{H-4'/H-5'} value of each stable conformer was calculated with the Karplus

Model 1 is a C4'-hydroxy derivative roridin H.²⁶ Notably, the C12' in roridin H was reported to resonate at 18.2 ppm, which is 5.1 ppm

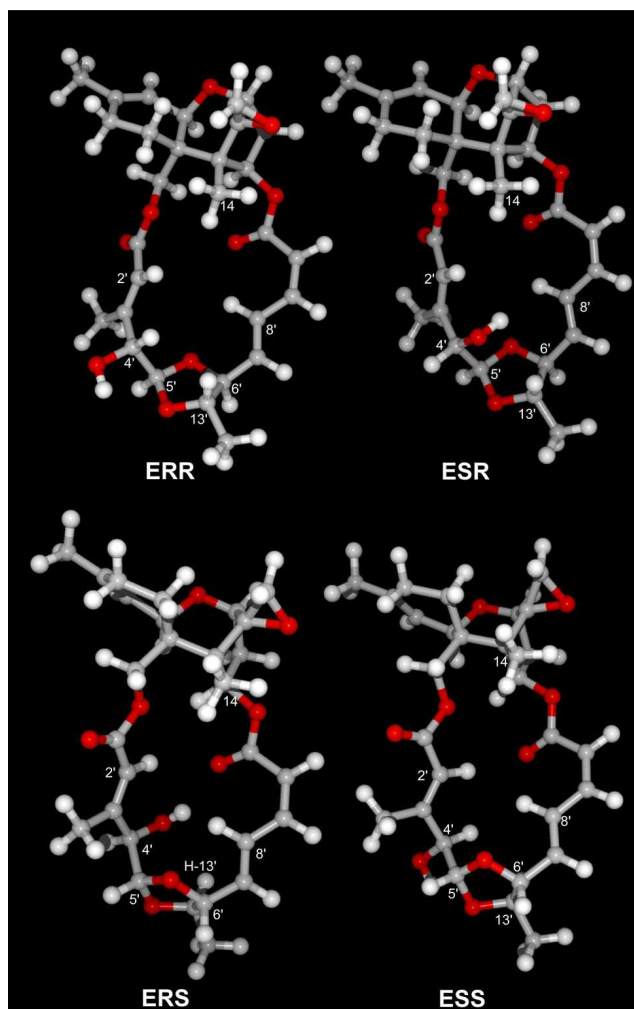


Figure 4. The most stable conformers of models **ERR**, **ERS**, **ESR**, and **ESS** based on ω B97X-D/6-31G*.

equation modified by Haasnoot.^{23,24} In contrast, the $^3J_{\text{H-4'/H-5'}}$ value for model **ESR** was estimated to be 1.7 Hz. Although model **ESS** shows a desirable $^3J_{\text{H-4'/H-5'}}$ value (6.2 Hz), this model disagrees with the transannular NOEs, as described. These results suggested model **ERR** to be the most plausible isomer as **1**.

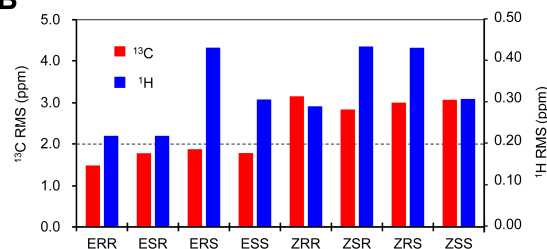
Next, we investigated with the theoretical chemical shifts employing ω B97X-D/6-31G*. The accuracy levels of the δH and δC RMS values in these calculations were set to be around 0.20 and 2.0 ppm, respectively, on the basis of our experience.^{21,22,25} The best candidate model **ERR** affords agreeable both theoretical ^1H and ^{13}C chemical shifts (0.22 and 1.49 ppm, respectively; bar chart **B**). Since these values for C4'-epimeric model **ESR** are also acceptable (0.22 and 1.78 ppm, respectively), this model can not be discarded with this argument. However, models **ERS** and **ESS**, the diastereomer around the C6'OC7'C12'O dioxolane ring moiety, yields large unacceptable ^1H RMS values (0.43 and 0.31 ppm, respectively).

Because we revised the (2'Z) double bond of **1'** to the (2'E) with the NOE experiments, a series of the (2'Z) isomeric models was also calculated. As expected, the C12' resonances of the (2'Z) isomers would appear at a remarkably higher frequency (22.3–26.2 ppm) than the experimental data (13.26 ppm), while those in all (2'E) isomeric models are agreeable (14.7–16.4 ppm; Table **A**). Furthermore, none of the (2'Z) isomeric models satisfy the ^1H or ^{13}C RMS values (>0.29 and >2.84 ppm, respectively). These results verified our previous conclusion, and revealed that

A

models	configurations					Boltzmann weighted calculated values	
	2'	4'	5'	6'	13'	$^3J_{\text{H-4'/H-5'}}$ (Hz)	$\delta_{\text{C-12'}}$ (ppm)
ERR	E	R	R	S	S	5.9	15.8
ESR	E	S	R	S	S	1.7	16.4
ERS	E	R	S	R	R	1.2	15.0
ESS	E	S	S	R	R	6.2	14.7
ZRR	Z	R	R	S	S	3.3	25.7
ZSR	Z	S	R	S	S	3.1	22.3
ZRS	Z	R	S	R	R	1.1	26.2
ZSS	Z	S	S	R	R	3.9	23.9
1						7.0	13.26

B



C

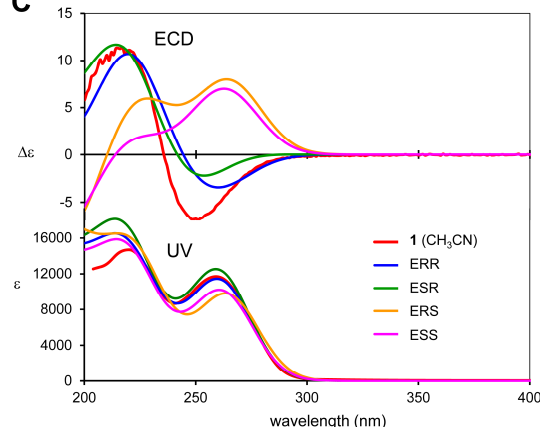


Figure 5. Summary of molecular modeling calculations. Table **A**: configurations of the isomers investigated and $^3J_{\text{H-4'/H-5'}}$ as well as $\delta_{\text{C-12'}}$ of the models. Bar chart **B**: $\delta^1\text{H}$ and $\delta^{13}\text{C}$ root-mean-square (RMS) values of the models against the experimental data in CDCl_3 . Spectra **C**: Theoretical ECD and UV spectra of the models. Calculations for Table **A** and bar charts **B** were generated with ω B97X-D/6-31G*, and spectra **C** was obtained using BHLYP/def2-TZVP// ω B97X-D/6-31G*.

larger than that of **1**. We assume that the C4'-hydroxy group contributes to a magnetic shielding of the C12' in addition to the steric compression by C1' carbonyl. This shielding can be explained by the γ -gauche effect.²⁷ In fact, the C12'-C3'-C4'-O adopts gauche conformation in the most stable conformer of model **ERR**. Similarly, the C12' resonance in model **ESS** can be explained. However, quantitative argument such as additivity of these shielding effects would be improper, because the C4'OH also affects to the distance between the C12' and the C1'-carbonyl.

Roridin J (**1**) shows negatively split Cotton effects ($\Delta\epsilon$ -6.7 at 251 nm and $+11.8$ at 218 nm) in CH_3CN . The theoretical ECD spectra for models **ERR** and **ESR** are similar each other and show accordance with the experimental spectrum (spectra **C**). Models **ERS** and **ESS** also afford resembled theoretical ECD spectra to each other, however, these do not match to the

experimental spectra at all. Molecular modeling calculations have suggested that the configurations at the C4' hardly contribute to the conformation of the macrocyclic ring. Since models giving resembled theoretical ECD spectra were found to adopt the resembling conformations around the macrocyclic moiety, it is likely that the experimental Cotton effects are attributed to an exciton coupling due to chiral torsion between the C1'–C3' enonate and the C7'–C11' dienolate chromophores.

As described, only model **ERR** satisfies spectroscopic properties of **1**, such as the NOEs, the $^3J_{\text{H-4'/H-5'}}$ value, the ^1H and ^{13}C NMR chemical shifts, and the ECD spectrum, and shows no inconveniences so far we investigated.

Fortunately, standing a solution of **1** in 1:1 mixture of hexane and ethyl acetate afforded yellowish plate crystals (m.p. 267–270 °C), which enabled an X-ray crystallographic analysis (**Figure 6**). Although the absolute structure could not be discussed because of high standard uncertainty in the Flack parameter ($\chi = 0.0(7)$), that confirmed not only the identical relative configuration but also nearly the same conformation as that of the most stable conformer obtained by the calculations. This result also demonstrated the high quality of molecular

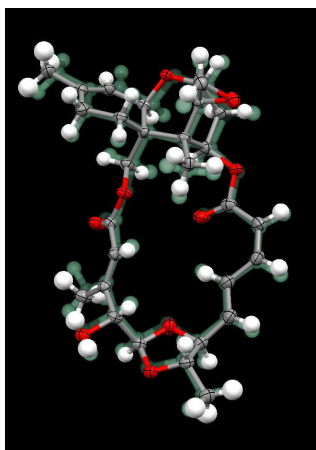


Figure 6. The X-ray crystallographic structural image of **1** (CPK colored ellipsoid model) overlaid on the most stable conformer of model **RRR** based on wB97X-D/6-31G* (green colored shadowed model). The X-ray image was inverted from the original data.

modeling in the present study.

3. Conclusion

As described, we revised a geometry at the 2',3'-double bond in the original structure of roridin J (**1'**) reported in 1980. Although the configurations of the stereogenic centers on the macrocyclic ring had remained unknown, this study established them to disclose the whole structure as **1** by a combination of a comprehensive NMR analysis and modeling calculations. All of the configurations were confirmed by an X-ray diffraction analysis.

4. Experimental

Fungus.

Calcarisporium arbuscula strain 1310-04 was isolated from a fruit body of *Gymnopilus junonius* which was collected at Aomori prefecture Japan in September 2013. It has been

deposited in the NITE Biological Resource Center (NBRC) under accession number NBRC 112400.²⁸

Isolation

The fungus *C. arbuscula* was cultured with a potato–dextrose medium [prepared from potato (2.0 kg), glucose (200 g), and H₂O (10.0 L)] at 25 °C by shaking (110 rpm) for 14 days. After mycerium was removed by filtration in suction, the filtrate was concentrated until the whole volume became 2.0 L. The resulting broth was shaken with EtOAc (1.0 L ×3), and the EtOAc layer was concentrated in vacuum to give the crude residue (3.0 g). The crude residue was suspended with 20% aqueous MeOH (10 mL) and loaded on Sep-Pack ODS (10 g). After washing with 20% aqueous MeOH (60 mL), elution with 40% aqueous MeOH afforded a fraction containing roridins (280 mg after concentration). Preparative HPLC [Sunfire Prep C18 OBD 19 mm × 150 mm, CH₃CN–H₂O (containing 0.1% TFA), 10 mL/min flow, detected at 254 nm] gave roridin J (**1**, 15 mg) and epiisororidin E (**2**, 62 mg).

Roridin J (1): m.p. 267–270 °C (from EtOAc/hexane), UV (6.3 × 10⁻⁵ mol/L, CH₃CN) λ_{max} 205 nm (ϵ 15000), 260 nm (ϵ 12000), ECD (6.3 × 10⁻⁵ mol/L, CH₃CN) $\Delta\epsilon_{235}$ 0, $\Delta\epsilon_{217}$ +11.5 $\Delta\epsilon_{251}$ -6.9, ^1H NMR (500 MHz, CDCl₃) δ 0.85 (3H, s, H₃₋₁₄), 1.37 (3H, d, J = 6.0 Hz, H_{3-14'}), 1.71 (3H, s, H₃₋₁₆), 1.81–2.05 (4H, H₂₋₇, H₂₋₈), 2.18 (1H, dt, J = 4.5, 15.3 Hz, H _{β -3}), 2.27 (3H, d, J = 1.0 Hz, H_{3-12'}), 2.47 (1H, dd, J = 8.5, 15.3 Hz, H _{α -3}), 2.82, 3.13 (each 1H, d, J = 4.0 Hz, H₂₋₁₃), 3.65 (1H, brd, J = 4.3 Hz, H-11), 3.65 (1H, dq, J = 8.9, 6.0 Hz, H-13'), 3.84 (2H, H-2, H-4'), 4.02 (1H, d, J = 12.5 Hz, H₂₋₁₅), 4.09 (1H, dt, J = 2.0, 8.9 Hz, H-6'), 5.25 (1H, d, J = 7.0 Hz, H-5'), 5.44 (1H, brd, J = 4.3 Hz, H-10), 5.76 (1H, brq, J = 1.2 Hz, H-2'), 5.80 (1H, d, J = 11.5 Hz, H-10'), 5.89 (1H, dd, J = 4.5, 8.5 Hz, H-4), 5.92 (1H, dd, J = 2.0, 15.5 Hz, H-7'), 6.55 (1H, t, J = 11.5 Hz, H-9'), 7.65 (1H, dddd, J = 0.9, 2.0, 11.5, 15.5 Hz, H-8') ^{13}C NMR (125 MHz, CDCl₃) δ 7.36 (C14), 13.05 (C12'), 15.94 (C14'), 20.34 (C7), 2¹⁹3.34 (C16), 27.60 (C8), 34.69 (C3), 43.20 (C6), 47.96 (C13), 49.15 (C5), 63.40 (C15), 65.55 (C12), 67.82 (C11), 73.80 (C4), 76.42 (C13'), 79.16 (C2), 79.74 (C4'), 82.23 (C6'), 103.29 (C5'), 118.61 (C10), 118.75 (C10'), 119.91 (C2'), 126.07 (C8'), 134.48 (C7'), 140.50 (C9), 143.11 (C9'), 155.26 (C3'), 165.90 (C1'), 166.21 (C11'). The ^1H and ^{13}C data were coincident with those in the literature. ESIMS (rel. int. %) m/z 551.2282 (25, calcd. for C₂₉H₃₆O₉Na [M+Na]⁺: 551.2257, 546.2731 (100, calcd. for C₂₉H₄₀NO₉ [M+NH₄]⁺: 546.2703), and 529.2467 (67, calcd. for C₂₉H₃₇O₉ [M+H]⁺: 529.2438). The ^1H and ^{13}C NMR data of this sample were coincident with those reported by Jarvis.¹⁴

Epiisororidin E (2): UV (5.1 × 10⁻⁵ mol/L, CH₃CN) λ_{max} 220 nm (ϵ 22000), 258 nm (ϵ 14000), ECD (5.1 × 10⁻⁵ mol/L, CH₃CN) $\Delta\epsilon_{233}$ 0, $\Delta\epsilon_{218}$ +13.8, $\Delta\epsilon_{249}$ -11.3, ^1H NMR (500 MHz, CDCl₃) δ 0.80 (3H, s, H₃₋₁₄), 1.15 (3H, d, J = 6.5 Hz, H_{3-14'}), 1.55 (1H, dd, J = 4.9, 13.0 Hz, H-7), 1.71 (3H, s, H₃₋₁₆), 2.02 (2H, m, H _{β -3}, H-8), 2.10 (1H, m, H-8), 2.12 (1H, dd, J = 6.0, 13.0 Hz, H-7), 2.23 (3H, d, J = 1.2 Hz, H_{3-12'}), 2.34 (1H, dt, J = 7.6, 13.0, H-4'), 2.56 (1H, dd, J = 8.2, 14.9, H _{α -3}), 2.56 (1H, m, H-4'), 2.84, 3.15 (each 1H, d, J = 4.0 Hz, H₂₋₁₃), 3.6 (1H, ddd, J = 5.0, 7.6, 10.2 Hz, H-5'), 3.75 (1H, dt, J = 7.6, 10.2 Hz, H-5'), 3.85 (1H, d, J = 5.0 Hz, H-2), 3.92 (1H, ddd, J = 1.0, 3.2, 6.1, H-6'), 4.01 (1H, dq, J = 3.2, 6.5 Hz, H-13'), 4.05, 4.20 (each 1H, d, J = 12.5 Hz, H₂₋₁₅), 4.06 (1H, brd, J = 5.8 Hz, H-11), 5.50 (1H, brdd, J = 1.2, 5.8 Hz, H-10), 5.82 (1H, d, J = 11.1 Hz, H-10'), 5.86 (1H, d, J = 1.2 Hz, H-2'), 5.9 (1H, dd, J = 6.1, 18.0 Hz, H-7'), 6.32 (1H, dd, J = 4.1, 8.2 Hz, H-4), 6.62 (1H, t, J = 11.1 Hz, H-9'), 7.56 (1H, dd, J = 11.1, 16.0 Hz, H-8') ^{13}C NMR (125 MHz, CDCl₃) δ 6.48 (C14), 17.87 (C14'), 19.23 (C12'), 22.35 (C7), 23.23 (C16), 27.68 (C8), 36.40 (C3), 40.32 (C4'), 42.59

(C6), 47.81 (C5), 48.48 (C13), 64.29 (C15), 65.65 (C12), 66.28 (C5'), 67.06 (C11), 68.48 (C13'), 75.06 (C4), 79.24 (C2), 81.83 (C6'), 117.24 (C2'), 118.82 (C10), 119.06 (C10'), 131.05 (C8'), 134.68 (C7'), 140.26 (C9), 142.33 (C9'), 157.99 (C3'), 166.35 (C1'), 166.42 (C11'), ESIMS (rel. int. %) m/z 537.2460 (45, calcd. for $C_{29}H_{38}O_8Na$ [M+Na]⁺: 537.2464), 532.2905 (100, calcd. for $C_{29}H_{42}NO_8$ [M+NH₄]⁺: 529.2910), 515.2640 (27, calcd. for $C_{29}H_{39}O_8$ [M+H]⁺: 515.2645). The ¹H and ¹³C NMR data of this sample were coincident with those reported by Jarvis.¹⁶

Verrucarol (4,15)-O-bis(2-naphthoate) **4** from epiisororidin E (**2**)

Epiisororidin E (**2**, 10 mg) was stirred with K₂CO₃ (20 mg) in MeOH (1.0 mL) at room temperature for 2 h. The suspension was diluted with diethyl ether (5.0 mL) and then filtered. The filtrate was concentrated in vacuum and then subjected to preparative silica gel TLC. Development with EtOAc:hexane (80:20) afforded **3** (4.5 mg; R_f = 0.2 under the above conditions). [α]_D²² = -31.5° (c 0.41 CHCl₃), (lit: [α]_D²¹ -40.6 (c 0.13, CHCl₃).¹⁹ ¹H NMR (500 MHz, CDCl₃) δ 0.95 (3H, s, H₃₋₁₄), 1.36 (1H, br, alcoholic proton at C15O), 1.66 (1H, brd, J = 9.1 Hz, alcoholic proton at C4O), 1.72 (3H, s, H₃₋₁₆), 1.74 (1H, dt, J = 1.8, 5.5 Hz, H-7), 1.91 (1H, ddd, J = 3.0, 5.5, 15.5 Hz, H $_{\beta}$ -3), 1.96 (1H, dd, J = 6.0, 12.3 Hz, H-7), 2.05 (2H, m, H-8), 2.58 (1H, dd, J = 7.5, 15.5 Hz, H $_{\alpha}$ -3), 2.81, 3.11 (each 1H, d, J = 3.9 Hz, H₂₋₁₃), 3.57, 3.76 (each 1H, d, J = 11.7 Hz, H₂₋₁₅), 3.62 (1H, d, J = 5.4 Hz, H-11), 3.82 (1H, d, J = 5.5 Hz, H-2), 4.63 (1H, br, H-4), 5.43 (1H, d, J = 5.4 Hz, H-10), ¹³C NMR (125 MHz, CDCl₃) δ 7.29 (C14), 20.99 (C7), 23.28 (C16), 28.25 (C8), 39.96 (C3), 43.89 (C6), 47.64 (C13), 49.00 (C5), 62.55 (C15), 65.71 (C12), 66.54 (C11), 74.56 (C4), 78.67 (C2), 118.77 (C10), 141.05 (C9), ESIMS (rel. int. %) m/z 289.1408 (66, calcd. for $C_{15}H_{22}O_4Na$ [M+Na]⁺: 289.1416), 267.1585 (60, calcd. for $C_{15}H_{23}O_4$ [M+H]⁺: 267.1596), and 249.1485 (100, calcd. for $C_{15}H_{21}O_3$ [MH-H₂O]⁺: 249.1491). The ¹H and ¹³C data were coincident with those in the literature.¹⁹

Verrucarol (**3**) (1.0 mg) thus prepared was stirred with 2-naphthoyl chloride (5.0 mg) and *N,N*-dimethyl-4-aminopyridine (DMAP, 4.0 mg) in CH₂Cl₂ (0.2 mL) at room temperature for 30 min. Diethyl ether (5.0 mL) was added to the mixture, and the resulting suspension was filtered through a cotton filter. After concentration *in vacuo*, the residue was purified using silica gel column chromatography (EtOAc:hexane = 33:67) to give the bis(2-naphthoate) **4** (1.6 mg, R_f = 0.45 under the above conditions, and the quantity of the sample was estimated by assuming its ϵ value at 236 nm to be 135000). ECD (7.0×10^{-6} mol/L, CH₃CN) $\Delta\epsilon_{242}$ +6.8, $\Delta\epsilon_{229}$ -20.2, ¹H NMR (500 MHz, CDCl₃) δ 1.13 (3H, s, H₃₋₁₄), 1.75 (3H, s, H₃₋₁₆), 1.98-2.12 (3H, m, H-7, H-8), 2.18 (1H, dd, J = 6.0, 11.6 Hz, H-7), 2.26 (1H, ddd, J = 3.5, 5.3, 15.5 Hz, H $_{\beta}$ -3), 2.77 (1H, dd, J = 7.5, 15.5 Hz, H $_{\alpha}$ -3), 3.00, 3.26 (each 1H, d, J = 4.1 Hz, H₂₋₁₃), 3.91 (1H, d, J = 5.4 Hz, H-11), 3.97 (1H, d, J = 5.3 Hz, H-2), 4.42, 4.64 (each 1H, d, J = 12.3 Hz, H₂₋₁₅), 5.53 (1H, dd, J = 1.5, 5.4 Hz, H-10), 6.05 (1H, dd, 3.5, 7.5 Hz, H-4), 7.50-7.60 (4H, aromatic protons), 7.83-7.88 (4H, aromatic protons), 7.94, 7.97 (each 1H, brd, J = 8.0 Hz, aromatic protons), 8.01, 8.06 (each 1H, dd, J = 1.4, 8.4 Hz, aromatic protons), 8.58, 8.60 (each 1H, brs, aromatic protons). ESIMS (rel. int. %) m/z 597.2245 (33, calcd. for $C_{37}H_{34}O_6Na$ [M+Na]⁺: 597.2253), 592.2683 (54, calcd. for $C_{37}H_{38}NO_6$ [M+NH₄]⁺: 592.2699), and 575.2421 (100, calcd. for $C_{37}H_{35}O_6$ [M+H]⁺: 575.2434).

Preparation of **4** from roridin J (**1**)

In the same manner as above, roridin J (**1**, 1.5 mg) was treated with K₂CO₃ (10 mg) in MeOH (0.5 mL). The similar workup and purification gave **3** (approximately 1.5 mg). The ¹H NMR spectrum of the crude sample agreed with that of the sample

prepared from epiisororidin E (**2**). The obtained sample was 2-naphthoylated under the conditions similar to those mentioned above by employing 2-naphthoyl chloride (2.0 mg), DMAP (2.0 mg), and CH₂Cl₂ (0.5 mL). Then, a workup similar to that discussed above and the following preparative silica gel TLC under the same conditions afforded the bis(2-naphthoate) **4** (0.6 mg, the quantity was estimated by assuming its ϵ value at 236 nm to be 135000). ECD (7.0×10^{-6} mol/L, CH₃CN) $\Delta\epsilon_{242}$ +6.8, $\Delta\epsilon_{229}$ -20.2. The chromatographic property and the ECD profile of this sample were identical to those derived from **2**.

Modeling calculations

Eight isomeric models, namely **ERR**, **ESR**, **ERS**, **ESS**, **ZRR**, **ZSR**, **ZRS**, and **ZSS**, were constructed using Spartan'14. The three letters for the models refer to the configurations at the 2', 4', and 5' positions, respectively. A conformational search for each model was performed using MMFF by setting the rotation at C15-O bonding, and the flips at C1', C2', C3', C4', C5', C7', C8', C9', C10', and C11', which theoretically generate 354294 initial conformers and the search gave 100 candidates of stable conformers in each model. In some models, the program automatically judged the completion of the search to terminate after checking approximately 1×10^4 conformers. The candidates were refined with HF/STO-3G. After removing the overlaps, conformers (4-9 conformers) within 10 kJ/mol from the global minimum conformer were further optimized stepwise by EDF2/6-31G* and ω B97X-D/6-31G* on Spartan'14 and Spartan'16, respectively, considering the entropy term using a vibrational analysis (the software was updated during the research period). The optimized conformers were subjected to chemical shift calculations with the ω B97X-D/6-31G*. Distributions of the conformers were estimated based on the relative free energies (ΔG) and the Boltzmann distribution law. Theoretical chemical shifts were corrected based on the distributions of the conformers. Major conformers existing in cumulatively 90 % populations of models **ERR**, **ESR**, **ERS**, and **ESS** were subjected to ECD calculations on Turbomole X (version 7.1) with def2-TZVP/BH-LYP// ω B97X-D/6-31G*. Fifty excitations were examined to express the UV and ECD spectra in the range 200-600 nm. The UV and ECD spectra of each conformer were constructed based on the frequencies as well as the oscillator strength and the rotary strength, respectively, by employing the NORMDIST function in Microsoft Excel® 2016 (standard deviation = 14 nm for UV spectra; 15 nm for ECD spectra). The wavelengths for these spectra were corrected (+14 nm) based on the experimental UV absorption of **1**. Theoretical UV and ECD spectra were obtained after correction based on the conformational distributions. The theoretical UV intensity of model **ERR** was normalized with experimental data at 260 nm, and the same parameter was used for the other models. The intensities of the theoretical ECD spectra were appropriately adjusted.

X-ray diffraction analysis²⁵

A solution of **1** (approximately 10 mg) in a mixture of 1:1 EtOAc and hexane (0.3 mL) was stood at room temperature for a week to precipitate the crystalline. After the mother liquid was pipetted off, diethyl ether (0.2 mL) was added and the mixture was gently agitated for 10 second at room temperature. The ethereal liquid was quickly removed by pipetting to give the yellowish single crystals. Data were collected at 123 K on a Rigaku RAXIS RAPID II imaging plate diffractometer using graphite-monochromated Mo K α radiation (λ = 0.71075 Å) and corrected by the Lorentz, polarization, and absorption effects. The structure was solved by direct methods (SHELXS-97) and refined on F^2 using the full-matrix least-squares method

(SHELXS-97).²⁹ Anisotropic refinement was applied to all non-hydrogen atoms. All hydrogen atoms were located at the calculated positions. Crystallographic data were deposited at the Cambridge Crystallographic Data Centre (CCDC-1556402). The data can be obtained free of charge from the Cambridge Crystallographic Data Centre.

Acknowledgment

Part of this research was supported by a Grant-in-Aid for Scientific Research (B) (15H04491) and a Grant-in-Aid for Challenging Exploratory Research (16K14910) from the Japan Society for the Promotion of Science (JSPS). We would like to thank Enago (www.enago.jp) for the English language review.

Supplementary Material

Supplementary Material associated with this article can be found in the online version at <http://>

References and Notes

1. Tamm, C. In *Fortschritte der Chemie Organischer Naturstoffe / Progress in the Chemistry of Organic Natural Products*; Herz, W.; Grisebach, H.; Kirby, G. W. Eds.; Springer Vienna, 1974; pp. 63-117.
2. Matsumoto, M.; Hiroshi, M.; Uotani, N.; Matsumoto, K.; Kondo, E. *J. Antibiot.* **1977**, *30*, 681-682.
3. Kupchan, S. M.; Jarvis, B. B.; Dailey, R. G.; Bright, W.; Bryan, R. F.; Shizuri, Y. *J. Am. Chem. Soc.* **1976**, *98*, 7092-7093.
4. Kupchan, S. M.; Streelman, D. R.; Jarvis, B. B.; Dailey, R. G.; Sneden, A. T. *J. Org. Chem.* **1977**, *42*, 4221-4225.
5. Vittimberga, J. S.; Vittimberga, B. M. *J. Org. Chem.* **1965**, *30*, 746-748.
6. Zhang, S.-Y.; Li, Z.-L.; Guan, L.-P.; Wu, X.; Pan, H.-Q.; Bai, J.; Hua, H.-M. *Magn. Reson. Chem.* **2012**, *50*, 632-636.
7. Liu, J. Y.; Huang, L. L.; Ye, Y. H.; Zou, W. X.; Guo, Z. J.; Tan, R. X. *J. Appl. Microbiol.* **2006**, *100*, 195-202.
8. Saikawa, Y.; Okamoto, H.; Inui, T.; Makabe, M.; Okuno, T.; Suda, T.; Hashimoto, K.; Nakata, M. *Tetrahedron* **2001**, *57*, 8277-8281.
9. Amagata, T.; Rath, C.; Rigot, J. F.; Tarlov, N.; Tenney, K.; Valeriote, F. A.; Crews, P. *J. Med. Chem.* **2003**, *46*, 4342-4350.
10. Yu, N.-J.; Guo, S.-X.; Lu, H.-Y. *J. Asian Nat. Prod. Res.* **2002**, *4*, 179-183.
11. Wagenaar, M. M.; Clardy, J. *J. Antibiot.* **2001**, *54*, 517-520.
12. Kumari, I.; Ahmed, M.; Akhter, Y. *Appl. Microbiol. Biotechnol.* **2016**, *100*, 5759-5771.
13. Došen, I.; Andersen, B.; Phippen, C. B. W.; Clausen, G.; Nielsen, K. F. *Anal Bioanal Chem.* **2016**, *408*, 5513-5526.
14. Jarvis, B. B.; Stahly, G. P.; Pavanadasivam, G.; Mazzola, E. P. *J. Antibiot.* **1980**, *33*, 256-258.
15. Silverstein, R. M.; Webster, F. X.; Kiemle, D. J. *Spectrometric Identification of Organic Compounds* John Wiley & Son Inc.: Hoboken, 2005.
16. Jarvis, B. B.; Wang, S. *J. Nat. Prod.* **1999**, *62*, 1284-1289.
17. Ridge, C. D.; Mazzola, E. P.; Coles, M. P.; Hinkley, S. F. R. *Magnetic Resonance in Chemistry* **2016**, 337-340.
18. Gai, Y.; Zhao, L.-L.; Hu, C.-Q.; Zhang, H.-P. *Acta Crystallogr. Sect. E: Struct. Rep. Online* **2007**, *63*, o2990-o2991.
19. Ishihara, J.; Nonaka, R.; Terasawa, Y.; Shiraki, R.; Yabu, K.; Kataoka, H.; Ochiai, Y.; Tadano, K.-i. *J. Org. Chem.* **1998**, *63*, 2679-2688.
20. Gutzwiller, J.; Mauli, R.; Sigg, H. P.; Tamm, C. *Helv. Chim. Acta.* **1964**, *47*, 2234.
21. Tanaka, S.; Honmura, Y.; Uesugi, S.; Fukushi, E.; Tanaka, K.; Maeda, H.; Kimura, K.-i.; Nehira, T.; Hashimoto, M. *J. Org. Chem.* **2017**, *82*, 5574-5582.
22. Kusakabe, K.; Honmura, Y.; Uesugi, S.; Tonouchi, A.; Maeda, H.; Kimura, K.-i.; Koshino, H.; Hashimoto, M. *J. Nat. Prod.* **2017**, *80*, 1484-1492.
23. Haasnoot, C. A. G.; de Leeuw, F. A. A. M.; Altona, C. *Tetrahedron* **1980**, *36*, 2783-2792.
24. Stenutz, R., Conformational analysis of natural products, <http://www.stenutz.eu/conf/index.html>
25. Honmura, Y.; Uesugi, S.; Maeda, H.; Tanaka, K.; Nehira, T.; Kimura, K.-i.; Okazaki, M.; Hashimoto, M. *Tetrahedron* **2016**, *72*, 1400-1405.
26. Traxler, P.; Tamm, C. *Helvetica Chimica Acta* **1970**, *53*, 1846-1869.
27. Jacobsen, N. E. In *NMR Data Interpretation Explained: Understanding 1D and 2D NMR Spectra of Organic Compounds and Natural Products*; John Wiley & Sons Inc.: Hoboken, New Jersey, 2016; pp. 143-146.
28. <http://www.nbrc.nite.go.jp/e/index.html>.
29. (a) Sheldrick, G. M. SHELXS-97, Programs for Solving X-ray Crystal Structures; University of Göttingen, 1997. (b) Sheldrick, G. M. SHELXL-97, Programs for Refining X-ray Crystal Structures; University of Göttingen, 1997.